Indian Journal of Engineering & Materials Science
Vol. 21, October 2014, pp. 543-556

Optimization of cutting tool geometry based on flank wear – DoE, PSO and SAA approach

T Tamizharasan[a] & J Kingston Barnabas[b]*

[a]TRP Engineering College, Irungalur, Tiruchirappall 621 105, India

[b]Department of Mechanical Engineering, Anjalai Ammal Mahalingam Engineering College, Kovilvenni 614 403, India

Received 24 December 2012; accepted 3 April 2014

In this analysis, an attempt has been made to study the effects of included angle, hardness, rake angle, tool approach angle and nose radius of cutting inserts on flank wear with the surface roughness as constraint. The selected parameters are varied through three levels. A new parametric study without considering any kind of benchmark problems in this area is performed and methodology has been developed to analyze the effects of selected parameters on the flank wear of cutting insert. As per the L_{18} orthogonal array, the values of flank wear after machining are measured and recorded. The best levels of selected parameters for the minimization of flank wear are identified by using Taguchi's Design of Experiments. A validation experiment is conducted with the identified best levels of parameters, and the corresponding flank wear is recorded. Also this analysis inter-relates the performances of design of experiments (DoE), regression analysis, particle swarm optimization and simulated annealing algorithm (SAA) to obtain the best possible solution. The result of this analysis identifies the optimal values of selected parameters for effective and efficient machining. The experimental, optimized and predicted values of flank wear are compared and correlated for all the test conditions.

Keywords: Flank wear, Surface roughness, Taguchi's design of experiments, Particle swarm optimization, Simulated annealing algorithm

The selection of optimal geometry of cutting inserts for every machining process plays a major role in maintaining the quality of machined products. For maintaining higher production rates at minimum cost, optimization of cutting tool geometry is mandatory[1]. The influences of cutting tool edge geometry on many fundamental aspects such as cutting forces, chip formation, cutting temperature, tool wear, tool-life and characteristics like surface roughness and surface damage have been demonstrated in the experimental investigations[2,3]. Variation of machining parameters like cutting speed, feed and depth of cut can help in achieving the desired chip form in order to improve the productivity. But changing machining conditions to break the chip is usually not possible due to the requirements of the machining processes and their impact on tool life, cutting zone temperature and surface finish. Hence, the variation in the tool geometry is one of the important parameter to be considered for desirable chip form without hindering the turning performance[4].

Al-Zkeri *et al.*[5] investigated the effects of edge radius of a round-edge coated carbide tool on chip formation, cutting forces, and tool stresses in orthogonal cutting of an alloy steel 42CrMo4 (AISI 4142H). It was found from the experimental result that the cutting force is not significantly influenced by the cutting edge radius, but increasing the radius tends to slightly increase the feed force. On the rake face, the values of maximum tool temperature are predicted for all the cases modeled. It was observed that, the temperature increases with the increase of edge radius.

Baldoukas *et al.*[6] investigated the variation of tool rake angle on main cutting force during turning of different materials. The results of the investigation reveals that for AISI 1020 the main cutting force shows decreasing trend as the rake angle increases from 0º to 20º. But for UNS C23000 specimen, the main cutting force remains unchanged with variation in rake angle from 0º to 20º. Further, it was found that when the main cutting force and chip formation are considered together, the optimum value of rake angle for AISI 1020 material is γ = 12º and for UNS C23000 γ = 0º.

Neseli *et al.*[7] investigated the influence of tool geometry on the surface finish in turning of AISI 1040 steel. In order to find out the effect of tool

*Corresponding author (E-mail: kingstonmech@gmail.com)

geometry parameters on the surface roughness during turning, response surface methodology (RSM) was used. The results indicated that the tool nose radius was the dominant factor on the surface roughness. It was also found that there is a good agreement between the predicted and measured values of surface roughness.

Singh and Rao[8] carried out the experimental investigation to see the effect of the tool geometry (effective rake angle and nose radius) and cutting conditions (cutting speed and feed) on the surface finish during the hard turning of the bearing steel. First- and second-order mathematical models were developed in terms of machining parameters by using the response surface methodology on the basis of the experimental results. The surface roughness prediction model has been optimized to obtain the surface roughness values by using genetic algorithms. It was found that, the genetic algorithm program gives minimum values of surface roughness and their respective optimal conditions.

Choudhary and Chauhan[9] studied the machinability of aluminium alloy 7075 with the prime objective to ascertain the minimum tangential force and fine surface roughness. Series of tests were conducted in order to investigate the machinability with the objective to study the performance of different tool materials PCD and carbide. The main factors deciding the above objective are cutting speed, feed rate, depth of cut and approach angle. Here, an attempt had been made to model the machinability evaluation through face centred CCD of response surface method. The experimental results indicate that the proposed mathematical model suggested could adequately describe the performance of the factors that are being investigated. The results indicate that the polycrystalline diamond tool provide satisfactory results with better tool life than carbide tool at high speed turning.

Silva and Davim[10] compared the performance of uncoated carbide tools with standard cutting geometry and tools with modified edge preparation during precision turning of polyamide with and without 30% glass fiber reinforcing. The results indicated that, in general, the turning force components are reduced with the tool nose radius and the specific cutting force is decreased as feed rate is elevated, presenting values comparable to metallic alloys. It was also noticed that the surface roughness increased as feed rate is elevated and tool nose radius is reduced.

During the hard-turning process, complex and mutual interactions are created, at the contact surface, between tool and work-piece. Consequently, significant forces and high temperatures cause wear and sometimes breakage of the tool. Usually, such conditions lead to both contact surfaces being damaged. Moreover, the exactness of the geometrical shapes can be reduced or the mechanical characteristics modified.

Bhattacharyya *et al.*[11] studied the failure modes and the wear mechanisms operating at the tool faces, when machining Incoloy 901 with Syalon ceramic tools. It was found that at slower speeds, attrition is the dominant wear mechanism, whereas at higher speeds diffusion followed by plastic deformation dominates.

Barry and Byrne[12] investigated the mechanisms of alumina/TiC cutting tool wear in the finish turning of hardened steels with particular cognizance of the work material inclusion content. It was found from the investigation that, the rate of tool wear appears to be determined by the hard inclusion content or alloy carbide content of the work material.

Kharis and Lin[13] carried out the experimental investigation to study the tribological influences of PVD-applied TiAlN coatings on the wear of cemented carbide inserts and the microstructure wear behaviors of the coated tools under dry and wet machining. Micro-wear mechanisms were identified through SEM micrographs. It was found that these micro-structural variations of coatings provide structure-physical alterations as the measures for wear alert of TiAlN coated tool inserts under high speed machining of steels.

Meyer *et al.*[14] presented an experimental approach of modified corner radius geometry of cutting tools for hard turning processes. The size and direction of the contact length of the cutting edge as well as the load impact during machining are adjusted for the minimization of tool wear. The presented results show that the corner radius and the process parameters influence the tool wear progression over the operation time.

Singh and Khan[15] carried out the experimental studies to analyze the effect of varying cutting parameters including cutting speed, feed rate, depth of cut and cutting nose radius of insert on surface roughness and material removal rate. The results revealed that the feed rate and nose radius were the most influential factors on the surface roughness, and

material removal rate in CNC turning process is greatly influenced by depth of cut followed by cutting speed.

Kolahan *et al.*[16] studied to simultaneously model and optimize machining parameters and tool geometry in order to improve the surface roughness for AISI1045 steel. The important controlling process parameters and tool geometry in turning include rake angle, side cutting edge angle, end cutting edge angle, cutting speed and feed rate. In turn, depth of cut, nose radius and free angle are set as constant parameters. The results illustrate that feed rate has slightly more effect on the surface roughness than the cutting speed.

Kadirgama *et al.*[17] described the wear mechanism and tool life when machining Hastelloy C-22HS with coated carbide. The experiment was conducted using four different cutting tool materials to study the tool behavior, in terms of wear and tool life machining of Hastelloy C-22HS. It was found that, the flank wear decreases with the increase of cutting speed, feed rate and axial depth. The feed rate has the most dominant effect on the flank wear, followed by the cutting speed and axial depth.

From the literature review, the past researchers used many techniques for the optimization of cutting tool geometry with single tool grade. But in this research work, three different grades of cutting inserts were selected in order to investigate the effects of hardness of cutting insert over the flank wear. An attempt has been made in this analysis to study the effects of included angle (IA), hardness (H), rake angle (RA), tool approach angle (TAA) and nose radius (NR) of cutting inserts on the flank wear. The selected parameters are varied through three levels. EN 19 specimen of chemical composition C – 0.43%; Si – 0.11%; Mn – 0.68%; S – 0.036%; phosphorus – 0.036%; Ni – 0.04%; Cr – 1.12%; Mo – 0.2%; Cu – 0.04% which has wide application such as manufacturing automobile axle shafts, automobile worm shafts, crank shafts, connecting rods and to high tensile bolts and studs has been selected for this study. An objective function is formulated with constraint to identify the optimal levels of selected parameters using Taguchi's DoE.

Conventional optimization techniques like full factorial method, Taguchi's DoE, etc., are applicable only for specific optimization problems which are capable of identifying only the best levels of parameters for the calculation of local optimal solution. Consequently, non-traditional optimization techniques such as simulated annealing algorithm (SAA), particle swarm optimization (PSO) technique etc., were used in the optimization problem to obtain the global solution. Yang and Natarajan[18] carried out an experimental work in optimizing the machining parameters for the minimization of flank wear and cutting zone temperature. Raja and Baskar[19] determined the optimized cutting parameters using particle swarm optimization (PSO) technique. Vijayakumar *et al.*[20] used ant colony system for the optimization of multi-pass turning operations. The optimization problem in turning has been solved by genetic algorithms, Tabu search, simulated annealing and particle swarm optimization to obtain more accurate results[21]. Sardinas *et al.*[22] optimized cutting parameters in turning process genetic algorithm. Asokan *et al.*[23] optimized the surface grinding operations using particle swarm optimization technique. Antonio[24] reported on a study of an optimization model based on genetic algorithms (GAs). This GA method determines the combined effects of the input parameters to the optimal machining parameter. Davim[25] developed surface roughness prediction models using artificial neural network (ANN) to investigate the effects of cutting conditions during turning of free machining steel, 9SMnPb28k(DIN). It was found from the analysis that cutting speed and feed rate have significant effects in reducing the surface roughness, while the depth of cut has the least effect. The combination of fuzzy logic and genetic algorithm is used to construct model of a physical process including manufacturing process[26]. The author also presented the results of few case studies of modeling various manufacturing process using GA-fuzzy approaches. Kanthababu[27] suggested for the implementation of evolutionary algorithms in different research areas which hold promise for future applications.

So many optimization techniques were applied for the optimization of cutting parameters in machining of various materials, but most of the researchers had not focused towards the selection of practically used machine component for machining. This study presents the results of Taguchi's design of experiments, regression analysis, PSO and SAA. Hence in this study, the results of the analyses obtained by the said techniques are correlated with the experimental values.

It is clear that variation in tool geometry is one of the major parameters to be considered in order to

enhance the turning productivity in terms of flank wear and surface integrity. Therefore, a mathematical approach has attracted much attention as a method for obtaining optimized geometry of cutting insert for the minimization of flank wear. Hence in this research work, the best levels of parameters of tool geometry such as included angle, hardness, rake angle, tool approach angle and nose radius of cutting inserts are obtained to minimize the flank wear.

Optimization and Modeling Tools

The tools used in this study are, Taguchi's Design of Experiments, Particle Swarm Optimization and Simulated Annealing Algorithm for optimization, and Regression Analysis for developing empirical models.

Taguchi's design of experiments

The optimization of process and product parameters considerably improves the quality characteristics. When the number of parameters and levels increase, the conventional method involves one variable at a time, while keeping the other parameters at fixed levels. This method is generally time consuming and requires a considerable number of experiments to be performed[28]. The Taguchi method is an experimental design technique useful at reducing the number of experiments by using orthogonal arrays[29,30]. The minimum number of experiments to be conducted is calculated as:

$$\text{Minimum numbers of experiments} = [(3-1)\times 5]+1 = 11 \approx L_{18}$$

where, L is number of levels of parameters and P is number of parameters

In order to normalize the data, signal-to-noise (S/N) ratio values of flank wear are calculated.

S/N ratio for flank wear and surface roughness is calculated as:

$$S/N\ Ratio = -10\log_{10}\frac{1}{n}\sum \bar{y}^{2} \qquad \ldots (1)$$

where, n is the number of serials of experiment and $\bar{y}$ is the sum of squares of measured data.

An objective function is formulated with constraint to identify the optimal levels of selected parameters using Taguchi's design of experiments. Since the objective of this analysis is to minimize the flank wear, lower-the-better category is selected to calculate the S/N ratio. Since the S/N values are used, the larger value is normally taken as better performance characteristic. Therefore, the highest value of S/N ratio identifies the optimal level of the particular parameter. Also the surface roughness is fixed as constraint and the value of surface roughness of the finished component is not allowed to exceed 3 microns[31]. Finally, a validation experiment is conducted with all the identified optimal levels of parameters to confirm the optimality.

Regression analysis

In general, regression analysis is to estimate or to predict the unknown value of a variable from the known value of the other variable. It is one of the very important statistical tools which are extensively used in almost all engineering and technologies. The regression analysis confined to the study of only two variables at a time is termed as simple regression. But quite often, the values of a particular phenomenon may be affected by multiplicity of factors. The regression analysis for studying more than two variables at a time is known as multiple regression. Both linear and non-linear regression analysis were used in this analysis to develop the empirical model based on experimentally observed cutting zone temperature. The cutting zone temperature values predicted by the empirical model are correlated with the experimentally observed cutting zone temperature values for the trend correlation.

Particle swarm optimization (PSO)

The PSO is an adaptive algorithm based on a social-psychological metaphor; a population of individuals adapts by returning stochastically toward previously successful regions. Particle swarm has two primary operators: velocity and position update. During each generation each particle is accelerated towards the particles previously as well as globally in best position. At each iteration, a new velocity value for each particle is calculated based on its current velocity, the distance from its previous best position, and the distance from the global best position. The new velocity value is then used to calculate the next position of the particle. This process is then iterated until a minimum error is achieved.

The particles are manipulated as,

$$V_i^{k+1} = \left(C_1 x r_{i1}^k \left(P_i^k - X_i^k\right)\right) + \left(C_2 x r_{i2}^k \left(P_g^k - X_i^k\right)\right) \qquad \ldots (2)$$

and

$$X_i^{k+1} = X_i^k + V_i^{k+1} \qquad \ldots (3)$$

Values of C_1 and C_2 are constants. The Eq. (2) is used to determine the i^{th} particle's new velocity at

each iteration and Eq. (3) provides the new position of i^{th} particle, adding its new velocity to its current position. The flow chart showing the steps of PSO is shown in Fig. 1.

Simulated annealing algorithm (SAA)

The SAA is an algorithm exploiting the analogy between the cooling and freezing of metals in the process of annealing. This is one of the global optimization techniques. This algorithm accepts the solutions which move towards the objectives and in the other way, it perhaps with a probability. The global optimum for the problems with many degrees of freedom is achieved with SAA. Minimum free energy state during the thermodynamic cooling of molten metals is represented in the SAA. In each iteration, a point is created according to Boltzmann probability distribution and it is the basis for the working of SAA. The next point is selected and a slow simulated cooling process guarantees to achieve the global optimum point. The schedule of the SAA is solution representation and generation, solution evaluation, annealing schedule, computational consideration and performance of algorithm.

The SAA simulates the slow cooling process to achieve the minimum function value in a minimization problem. The cutting parameters are introduced with the concept of Boltzmann probability distribution and the cooling phenomenon is simulated.

Simulated annealing is a point by point method. The algorithm begins with an initial point and a high temperature '*T*'. A second point is created at random in the vicinity of the initial point and the difference in the function values (ΔE) at these two points is calculated. If the second point has a smaller function value, then that point is accepted and otherwise that point is accepted with the probability of exp ($-\Delta E\, T^{-1}$). This completes an iteration of this simulated annealing procedure. In the next generation, another point is created at random in the neighborhood of the current point and the Metropolis algorithm is used to accept or reject the point. In order to simulate the thermal equilibrium at every temperature, the number of points (n) is usually tested at a particular temperature, before reducing the temperature. The algorithm is terminated when a sufficiently small temperature is obtained or a small enough change in the function values is found. The flow chart showing the steps of SAA is shown in Fig. 2.

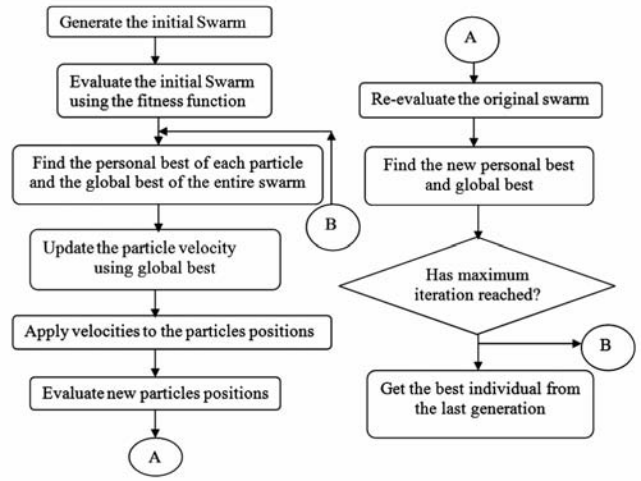

Fig. 1—Flowchart of PSO

Experimental Procedure

The wear of the cutting tool has direct impact on surface roughness of the finished product. Hence the flank wear is selected as objective with surface roughness as constraint. Main objective in this study

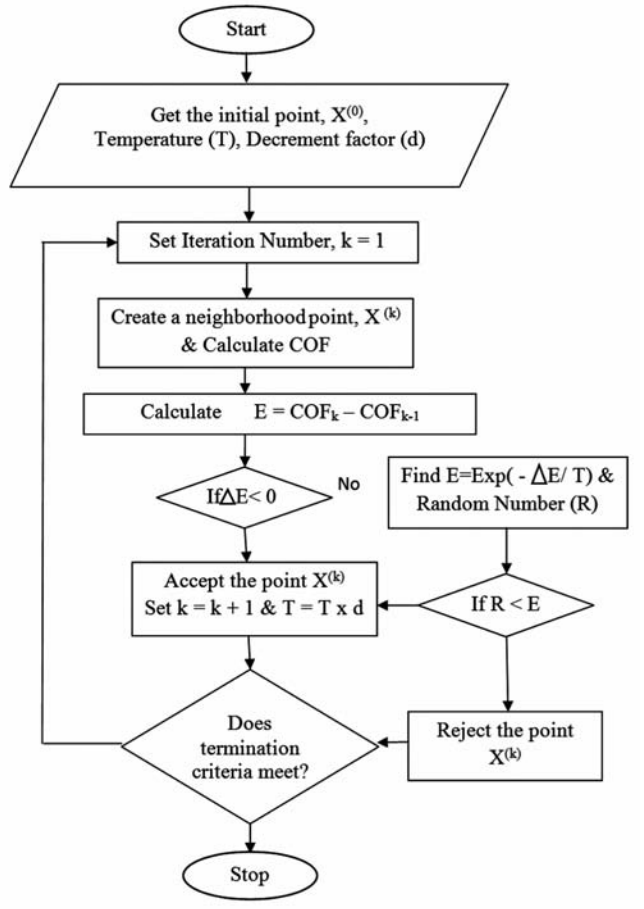

Fig. 2—Flowchart of SAA

is to optimize the geometry of cutting inserts like included angle of cutting insert, hardness of cutting insert, rake angle of cutting insert, tool approach angle and nose radius in order to reduce the flank wear of cutting tool. Some of the preliminary machining experiments were conducted before starting the actual experiment in order to identify the minimum and maximum value of included angle of cutting insert. When the included angle of cutting insert is lesser than 60^o and greater than 85^o, the results were not satisfactory to minimize the flank wear. Hence, the three shapes of cutting inserts selected are C, A and T which have the included angle (IA) of 80^o, 60^o and 85^o respectively which is in between the ranges of the values tested. Three grades of cutting inserts are selected such as SECO make, TeguTech and Kyocera. The hardness of these grades of cutting inserts were tested in Kidao Laboratory, Chennai for micro Vickers hardness test at 2 kg load and the average hardness values are 2340 Hv2, 2310Hv2 and 2290 Hv2 respectively. The rake angle values are selected based on the finishing grade of cutting insert such as MF2, MF3 and MF4 which have the rake angle of 25^o, 27^o and 29^o respectively.

Many researchers[14-16] studied the effects of included angle and nose radius of cutting insert on flank wear. Hence, as a parametric study, it is decided to include tool approach angle and nose radius as additional parameters in order to investigate the effects of the selected parameters on flank wear. Once again, the preliminary experiment was carried out to finalize the levels of tool approach angle and nose radius of cutting insert. The preliminary experiment results were found to be better for tool approach angle ranges from 60° to 90° and for nose radius ranges from 4 to 12 mm. The different levels and values of parameters selected are presented in Table 1.

Each machining operation is carried out for a determined duration of 300 s using CNC machine, irrespective of the number of passes in order to have the flank wear value within the safe limit of less than 0.4 mm. The experimental set-up during machining is shown in Fig. 3.

The specifications of CNC lathe, tool maker's microscope and surface roughness tester are presented in Table 2.

At the end of each experiment, the flank wear values of the cutting inserts are measured and recorded by using a tool maker's microscope of specifications shown in Table 2. Also the surface roughness of the finished product has been measured by using surface roughness tester of specifications presented in Table 2. The required experiments at different test conditions are performed with eighteen fresh cutting edges of same specifications. After completing the experiments, the arithmetic average surface roughness value of each machined surface is measured which is considered as a constraint not permitting to exceed 3 microns. The experimental test conditions and observed data of cutting zone temperature and surface roughness (raw and S/N Values) are presented in Table 3.

Results and discussion

The required experiments at different test conditions are performed with different fresh cutting edges. The values of flank wear of the cutting insert after the end of each experiment are measured and presented in Table 3. After completing the experiments, the arithmetic average surface roughness values of the finished rods are measured which is fixed as constraint and of not exceeding 3 microns. The S/N ratio values of the objective for the entire test conditions are calculated using Eq. (1) and the calculated values are also presented in Table 3. The

Table 1—The different levels and values of parameters selected

Included angle of cutting insert (IA)	80°	60°	85°
Hardness of cutting insert (H)	2340 Hv2	2310 Hv2	2290 Hv2
Rake angle of cutting insert (RA)	25°	27°	29°
Tool approach angle (TAA)	60°	75°	90°
Nose radius (NR)	4 mm	8 mm	12 mm

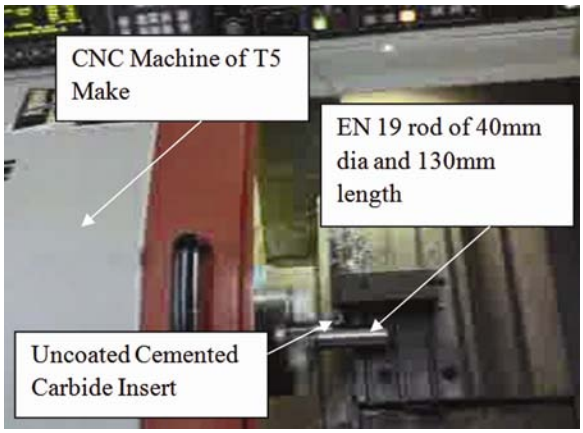

Fig. 3—Experimental set-up

Table 2—The specifications of materials

S.No.	Equipment/software	Description	Value/Range
1	CNC Lathe	Make	T-5
		Maximum speed	4500 rpm
		Max. swing	330mm
		Bar capacity	41mm
		X axis travel	230mm
		Z axis travel	230mm
		Chuck size	6”
2.	Tool maker’s microscope	model	1395A
		Magnification	30X (Standard)
		Objective	2X
		Working distance	80 mm (approx.)
		Image	Erect
		Observation	Monocular inclined at 30°
		Measuring stages	150 × 150 mm travel up to 25 mm in each direction having least count of 0.005 mm
3.	Surface Roughness Tester	Model	Surtronic 3+
		Traverse speed	1 mm/s
		Display	LCD matrix 2 lines × 16 characters, alphanumeric
		Parameters	R_a, R_q, R_z, R_y and S_m
		Calculation time	Less than reversal time

Table 3—Experimental test conditions and observed data

Test condition number	Included angle (degree)	Hardness (Hv2)	Rake angle (degree)	Tool approach angle (degree)	Nose radius (mm)	Flank wear (μm)	S/N FW	R_a (μm)	S/N R_a
1	80	2340	25	60	4	210	-46.44	2.08	-46.36
2	80	2310	27	75	8	245	-47.78	2.36	-47.45
3	80	2290	29	90	12	115	-41.21	1.02	-40.17
4	60	2340	25	75	8	195	-45.80	1.84	-45.29
5	60	2310	27	90	12	155	-43.80	1.42	-43.04
6	60	2290	29	60	4	230	-47.23	2.28	-47.15
7	85	2340	27	60	12	130	-42.27	1.28	-42.14
8	85	2310	29	75	4	140	-42.92	1.36	-42.67
9	85	2290	25	90	8	165	-44.34	1.56	-43.86
10	80	2340	29	90	8	100	-40.00	0.92	-39.27
11	80	2310	25	60	12	190	-45.57	1.78	-45.00
12	80	2290	27	75	4	250	-47.95	2.42	-47.67
13	60	2340	27	90	4	175	-44.86	1.62	-44.19
14	60	2310	29	60	8	205	-46.23	1.96	-45.84
15	60	2290	25	75	12	220	-46.84	2.16	-46.68
16	85	2340	29	75	12	90	-39.08	0.84	-38.48
17	85	2310	25	90	4	160	-44.08	1.48	-43.40
18	85	2290	27	60	8	185	-45.34	1.72	-44.71

best levels of selected parameters (maximum S/N ratio values) are identified as:

Included angle of cutting insert = 85° (IA_3)

Hardness of cutting insert = 2340 Hv2 (H_1)

Rake angle of cutting insert = 29° (RA_3)

Tool approach Angle = 90° (TAA_3)

Nose radius = 12 mm (NR_3).

With the identified best level of parameters, a validation experiment was conducted for obtaining the minimum value of flank wear. The value of flank wear observed from validation experiment is 85 μm which is lower than all the test condition values. The corresponding S/N ratio value of validation experiment is calculated using Eq. (1) and obtained as:

S/N flank wear = - 38.58

From Table 3, it is observed that, the minimum value of flank wear recorded is 90 μm for the test condition number 16. But when the validation experiment is conducted with the best levels of selected tool geometry parameters, the results show that there is a reduction of flank wear to some extent.

From Table 3, the % contribution of parameters on S/N-flank wear is calculated as:

Included angle –

$$Hardness\ of\ cutting\ insert\ \frac{-43.01}{-43.01-43.078-42.78-43.05-43.13}\times 100 = 20.00\% - 20.03\%$$

Hardness of cutting insert – 20.03%
Rake angle of cutting insert – 19.89%
Tool approach angle – 20.01%
Nose radius – 20.05%

From the above calculations, it is confirmed that the rake angle and tool approach angle are less significant on the S/N- flank wear followed by other parameters. The nose radius of cutting insert is highly significant on S/N-flank wear.

For verifying the validated results of flank wear with the linear regression model, the estimated mean of flank wear was calculated as:

$$FW_{em} = IA + H + RA + TAA + NR - 4FW_m \quad \ldots (4)$$

where,

FW_{em} = estimated mean of flank wear
IA = mean of flank wear corresponding to included angle of cutting insert
H = mean of flank wear corresponding to hardness of cutting insert
RA = mean of flank wear corresponding to rake angle of cutting insert.
TAA = mean of flank wear corresponding to tool approach angle
NR = mean of flank wear corresponding to nose radius
FW_m = overall mean of flank wear.

From Table 3, the mean values of the parameters are substituted in Eq. (4) and estimated mean of flank wear is calculated as:

FW_{em}= -43.01 – 43.07 – 42.78 – 43.05 – 43.13 – 4(-44.54)

FW_{em} = -36.88

The linear regression table for flank wear was developed by using regression analysis as shown in Table 4.

A confidence interval of 95% for the prediction of flank wear based on the validation experiment on the basis of linear regression model was obtained as:

$$CI = \sqrt{F_{0.05}(4, f_e)V_e\left[\frac{1}{n}+\frac{1}{R}\right]} \quad \ldots (5)$$

where,

f_e - error degrees of freedom (12) from Table 4
$F_{0.05}(4, f_e)$ - F ratio required for risk (4, 12) = 3.26 from standard "F" Table[32]
V_e - Error variance (1.571) from Table 4
R - Number of repetitions for confirmation test (1)
N - Total number of experiments = 18
n -Effective number of replications
=N / (1 + degrees of freedom associated with cutting zone temperature)
=18 / (1 + 17) = 1

By substituting the above values in Eq. (5), the value of confidence interval for flank wear based on linear regression model is calculated as:

CI= {3.26 x 1.571 [(1/1) + (1/1)]} $^{1/2}$
CI = 3.2004

The 95% confidence interval for the optimal flank wear in validation experiment was verified as,

$(FW_{em} - CI) < FW_{con} < (FW_{em} + CI)$

$(-36.8654 - 3.2004) < FW_{con} < (-36.8654 + 3.2004)$
$= -40.0658 < -38.5884 < -33.665$

The result of validation experiment shows that the flank wear is -38.0618 which is in between -40.0658 and -38.0618. The validated flank wear was thus confirmed by the above calculations. The regression model values are shown in Table 5.

The comparison of S/N ratio values of flank wear with linear regression model values is shown in Fig. 4.

Empirical equation for the flank wear based on linear regression model was developed as:

FW_{LR} = -193.579 + (0.093475×*IA*) + (0.049689×*H*) + (0.68373×*RA*) + (0.082211×*TAA*) + (0.306159×*NR*) … (6)

For verifying the validated results of flank wear with the non linear regression model, the estimated mean of flank wear was calculated as,

FW_{em} = -36.8654

The non linear regression data for flank wear was developed by using regression analysis as shown in Table 6.

Table 4—Summary output—linear regression – flank wear

ANOVA

	df	*SS*	*MS*	*F*	*Significance F*
Regression	5	95.79	19.15	12.19551	0.000231
Residual	12	18.85	1.571		
Total	17	114.65			

	Coefficients	Standard *Error*	*t Stat*	*P-value*
Intercept	-193.579	33.73	-5.73	9.34E-05
x IA	0.093475	0.027	3.41	0.005
x H	0.049689	0.014	3.45	0.004
x RA	0.683737	0.180	3.77	0.002
x TAA	0.082211	0.024	3.40	0.005
x NR	0.306159	0.090	3.38	0.005

Table 5—Regression model values of flank wear

Test condition number	S/N – FW	LR – FW	%error LR - FW	NLR - FW	%error NLR - FW
1	-46.44	-46.57	0.288	-46.64	0.420
2	-47.78	-44.24	7.999	-44.02	8.526
3	-41.21	-41.41	0.479	-41.52	0.756
4	-45.80	-45.99	0.412	-45.91	0.255
5	-43.80	-43.65	0.345	-43.97	0.384
6	-47.23	-48.19	1.998	-47.52	0.615
7	-42.27	-42.29	0.036	-42.36	0.200
8	-42.92	-43.63	1.630	-43.49	1.325
9	-44.34	-44.90	1.236	-44.70	0.799
10	-40.00	-40.15	0.380	-40.09	0.230
11	-45.57	-45.62	0.098	-45.96	0.843
12	-47.95	-46.46	3.220	-47.75	0.431
13	-44.86	-44.61	0.552	-44.92	0.142
14	-46.23	-45.97	0.556	-46.14	0.204
15	-46.84	-47.25	0.850	-46.89	0.096
16	-39.08	-36.69	1.534	-39.44	0.904
17	-44.08	-45.13	2.333	-44.51	0.976
18	-45.34	-46.00	1.434	-45.90	1.231

A confidence interval of 95% for the prediction of mean flank wear based on the validation experiment on the basis of non linear regression model was calculated as:

CI = 17.3498

The 95% confidence interval of the optimal flank wear in validation experiment was verified as,

(FW_{em} – *CI*) < FW_{con} < (FW_{em} + *CI*) (-36.8654 – 17.3498)< FW_{con} <(-36.8654 + 17.3498) -54.2152< -38.5884 < -19.5156

The result of validation experiment shows that the flank wear is -38.0618 which is in between -54.2152 and -19.5156. The validated flank wear was thus confirmed by the above calculations. The non-linear regression model values are shown in Table 5. The comparison of S/N ratio values of flank wear with non-linear regression model values is shown in Fig. 5.

Empirical equation for the flank wear based on non-linear regression model was developed as:

FW_{NLR}=(-582.551 - (3.60946x*IA*)+(0.195661x*H*) + (30.12142x*RA*)-(3.02699x*TAA*)+(15.02261x*NR*) + (0.00149x*IA*x*H*)+(0.007973x*IA*x*RA*)+(0.001054x*IA*x*TAA*)+(0.002484x*IA*x*NR*)-(0.01184x*H*x*RA*) + (0.00 1688x*H*x*TAA*) (0.00615x*H*x*NR*)-(0.033x*RA*x*TAA*)-(0.034x*RA*x*NR*) + (0.004x*TAA*x*NR*)) … (7)

By substituting the corresponding values of parameters corresponding to test condition number 6 in Eqs (6) and (7), the predicted values of flank wear were obtained as:

FW_{LR} = -48.1976
FW_{NLR} = -47.5270

An experimental value of flank wear corresponding to the same test condition number 6 is -47.2346.

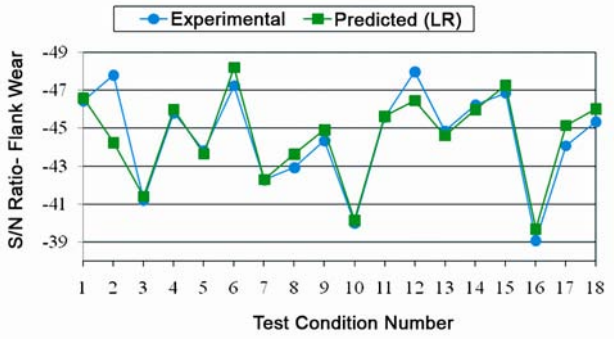

Fig. 4—Comparison of S/N ratio of flank wear with linear regression model values

The percentage deviation between the values of experimental flank wear and predicted flank wear were calculated and found as:

$\% FW_{LR} = 1.998\%$
$\% FW_{NLR} = 0.615\%$

Figure 6 shows the comparison between % error of flank wear in linear regression model with % error of flank wear in non-linear regression model.

The comparison between the average percentage deviation for the prediction of flank wear using LR and NLR is shown in Fig. 7.

The experimentally observed flank wear values are predicted using linear and non-linear regression analysis for all the test conditions. It is found from the experimental analysis that both linear and non-linear regression analysis predicted the values of flank wear closer to the experimentally collected values. But, the predicted values of flank wear using non-linear regression analysis very closely match with the experimentally observed values than that of linear regression analysis and it is well agreed with experimental work of Tamizharasan *et al*.[33] It is once again confirmed from Figs 6 and 7.

Since the traditional optimization technique, Taguchi's design of experiments identifies only the nearest levels of parameters, it is further decided to go for the non traditional optimization techniques such as particle swarm optimization technique and simulated annealing algorithm with non-linear regression empirical model, since the average percentage deviation from the experimentally obtained and predicted values of flank wear is lesser when compared with average percentage deviation using linear regression (Figs 6 and 7) in order to minimize flank wear by maintaining the value of surface roughness (constraint) well below 3.0 microns.

As a first attempt, the PSO technique is used to obtain the best global values of selected parameters. In PSO, the values of C_1 and C_2 in Eq. (2) are tried and the optimal values for both are found to be 3.

The different values of objective function (OF) by varying the number of populations using Eq. (6) are obtained as,

N = 10; OF = 0.72158
N = 15; OF = 0.70325
N = 20; OF = 0.70325
N = 25; OF = 0.70325
N = 30; OF = 0.70325
N = 35; OF = 0.70325
N = 40; OF = 0.70325

Table 6—Summary output – non-linear regression – flank wear

ANOVA

	df	*SS*	*MS*	*F*	*Significance F*
Regression	15	98.97	6.59	0.841	0.668097
Residual	2	15.67	7.839		
Total	17	114.65			

	Coefficients	*Standard Error*	*t Stat*	*P-value*
Intercept	-582.551	2058.50	-0.283	0.803
x IA	-3.60946	10.98	-0.328	0.773
x H	0.195661	0.848	0.230	0.839
x RA	30.12142	92.70	0.324	0.776
x TAA	-3.02699	10.37	-0.291	0.798
x NR	15.02261	38.68	0.388	0.735
x (IAxH)	0.00149	0.0046	0.321	0.778
x (IAxRA)	0.007973	0.052	0.151	0.893
x (IAxTAA)	0.001054	0.0066	0.159	0.888
x (IAxNR)	0.002484	0.026	0.095	0.932
x (HxRA)	-0.01184	0.038	-0.303	0.789
x (HxTAA)	0.001688	0.0047	0.358	0.754
x (HxNR)	-0.00615	0.016	-0.380	0.740
x (RAxTAA)	-0.03329	0.068	-0.486	0.674
x (RAxNR)	-0.03472	0.197	-0.175	0.876
x (TAAxNR)	0.004747	0.027	0.173	0.878

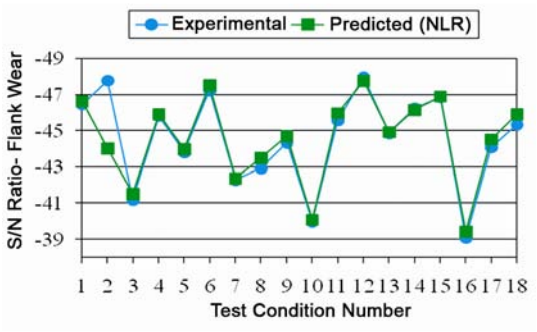

Fig. 5—Comparison of S/N ratio of flank wear with non-linear regression model values

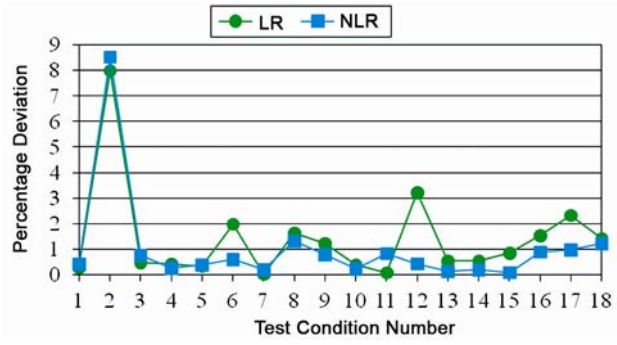

Fig. 6—Comparison of % error of LR flank wear and % error of NLR flank wear

N = 45; OF = 0.70325
N = 50; OF = 0.70325

From the above trials, it is found that for the population size of 15 the value of objective function is 0.70325 which lower than the values of objective function obtained from the trial with population size of 10. Also the values of objective function obtained from the trials with population sizes of 20, 25, 30, 35, 40, 45 and 50 are same as obtained with population size of 15. Hence the population size of 15 has been selected.

The best levels of parameters obtained using PSO based on non-linear regression empirical model and the corresponding S/N values of flank wear and surface roughness are presented in Fig. 8.

As a next attempt, the best values of selected parameters are obtained using SAA. In SAA, the initial temperature (T) and decrement factor (d) are the two important parameters which govern the successful working of the simulated annealing procedure. If a larger initial value of 'T' (or)'d' is chosen, it takes more number of iterations for convergence. On the other hand, if a small value of initial temperature 'T' is chosen, the search is not adequate to thoroughly investigate the search space before converging to the true optimum. Unfortunately, there are no unique values of the initial temperature (T), decrement factor (d) and number of iterations (n) that work for every problem. However, an estimate of the initial temperature can be obtained by calculating the average of the function values at a number of random points in the search space. A suitable value of 'n' can be chosen (usually between 2 and 100) depending on the available computing resource and the solution time. Decrement factor is left to the choice of the user. However, the initial temperature and subsequent cooling schedule require some trial and error efforts. Hence different combinations of these two parameters have been analyzed and the best results are obtained for the following combinations. There are better results for different possible combinations of these two parameters. But almost all the possible combinations have been tried out as:

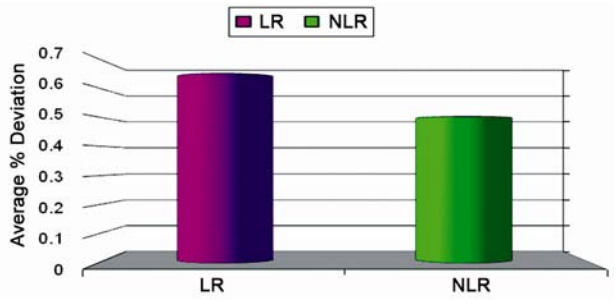

Fig. 7—Comparison between the average % deviation of linear regression and non-linear regression model values of flank wear

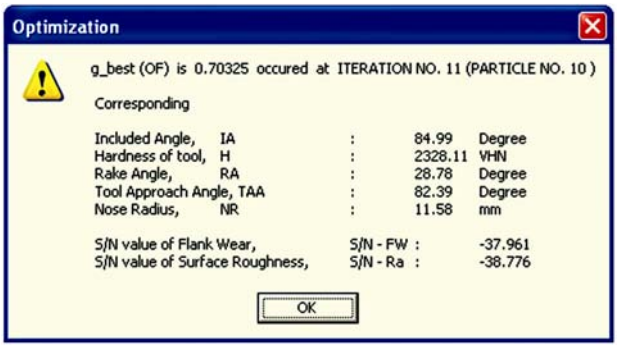

Fig. 8—Best levels of parameters obtained, S/N values of flank wear and surface roughness obtained from PSO using NLR

Number of iterations, n = 200 (convergence occurs at iteration number 44)

T = 500°C, df = 0.1 and OF = 0.69614
T = 500°C, df = 0.2 and OF = 0.69752
T = 500°C, df = 0.3 and OF = 0.69721
T = 500°C, df = 0.4 and OF = 0.696
T = 500°C, df = 0.5 and OF = 0.69779
T = 500°C , df = 0.6 and OF = 0.69574
T = 500°C, df = 0.7 and OF = 0.69811
T = 500°C, df = 0.8 and OF = 0.69745
T = 500°C, df = 0.9 and OF = 0.69745
T =1000°C, df = 0.8 and OF = 0.69745

From the various combinations, when the temperature and decrement factor are maintained at 500°C and 0.6, the minimum value of OF (0.69574) is obtained. The temperature of 1000°C does not improve the value of OF and hence, this temperature is not considered in this analysis.

The best levels of selected parameters obtained using SAA based on non-linear regression model and the S/N values of flank wear and surface roughness are presented in Fig. 9.

Itr. No.	IA	H	RA	TAA	NR	S/N	S/N	OF
Unit	Degree	Hv2	Degree	Degree	mm	FW	Ra	–
37	84.76	2339.59	25.30	89.84	11.24	-38.025	-36.879	0.70443
38	83.17	2339.80	25.03	89.72	11.92	-38.015	-36.825	0.70424
39	84.99	2338.44	25.18	89.98	11.35	-37.989	-36.848	0.70376
40	84.24	2338.95	25.23	89.87	11.97	-37.885	-36.715	0.70183
41	84.73	2338.65	25.08	89.88	11.82	-37.824	-36.665	0.70069
42	84.90	2339.30	25.01	89.68	11.91	-37.711	-36.548	0.69860
43	84.50	2339.49	25.03	89.99	11.93	-37.701	-36.527	0.69843
44	84.96	2339.87	25.01	89.94	11.97	-37.556	-36.383	0.69574
45								
46								

Minimum OF (0.69574) occured at ITERATION NO. 44

Fig. 9—Best levels of parameters obtained, S/N values of flank wear and surface roughness obtained from SAA using NLR

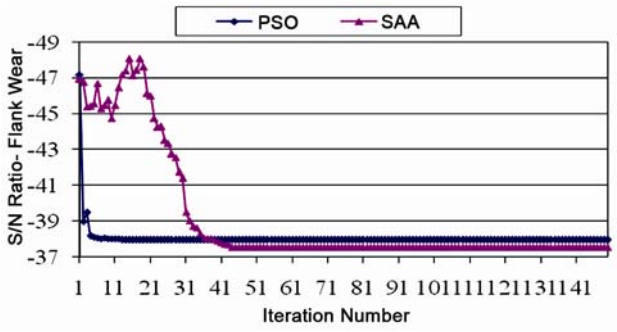

Fig. 10—Comparison of output of SAA and PSO on NLR empirical model based on flank wear

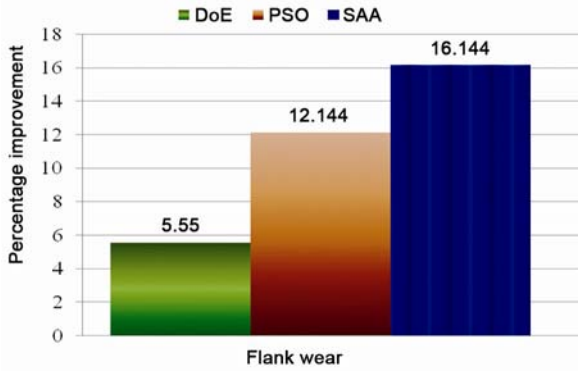

Fig. 11—Comparison of % improvement in objective using DoE, PSO and SAA

The comparison of output of SAA and PSO based on NLR empirical model based on flank wear is shown in Fig. 10.

It is found from Fig. 10, SAA optimize the selected parameters compared to Taguchi's DoE and PSO for the minimization of flank wear which is agreed with experimental work of Barnabas and Tamizharasan[31].

The percentage of improvement in flank wear with the application of Taguchi's design of experiments is calculated from the validated result and the minimum values of objectives from the Table 3 as,

The percentage of improvement in flank wear using DoE = [(90 -85) /90] ×100 = 5.55%

Similarly the percentage improvement in flank wear from the minimum value of flank wear from the Table 3 with the application of PSO and SAA are 12.144% and 16.144%, respectively. It is found that PSO gives minimum value of flank wear when compared with the value of flank wear obtained using Taguchi's DoE and it is having a good agreement with the results of past experimental work[34].

The percentage improvement in flank wear with the application of Taguchi's DoE, PSO and SAA is graphically represented in Fig. 11.

It was found from Table 3 that, when the tool approach angle is 60°, the flank wear values are high in almost all the test conditions except in test condition number 7 which may be due to the confusing chip flow which rubs over the nose of the cutting insert. This is once again confirmed by the flank wear structure captured by SEM for the test condition number 6 shown in Fig. 12a. When the tool approach angle is 90°, the flank wear values are low for the test condition numbers 3 and 10. The flank wear structure captured by SEM for the test condition number 3 shown in Fig. 12b.

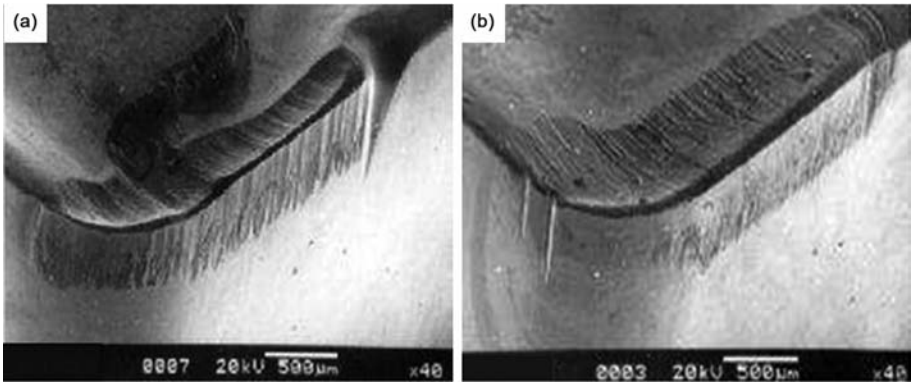

Fig. 12—Comparison of flank wear structure of cutting insert for two different levels of tool approach angle (a) test condition number 7 and (b) test condition number 3

Conclusions

The cutting tool edge geometry influences on the fundamental aspects such as flank wear and surface roughness etc. Hence, in this analysis, the effects of various cutting tool geometry such as included angle, tool grade, rake angle, tool approach angle and nose radius for the minimization of flank wear has been investigated.

It is observed from the analysis that when machining is carried out with the best levels of tool geometry parameters obtained using Taguchi's DoE, the flank wear is reduced by 5.55% when compared to the least tabulated values of flank wear recorded in Table 3.

It is found from the regression analysis that the average deviation of predicted values of flank wear from the experimentally observed flank wear using linear regression is 1.408%. But the average deviation of predicted values of flank wear from the experimentally observed flank wear using non-linear regression analysis is 1.019%. From the collected data, it is found that the non-linear regression model shows a comparatively minimum deviation of flank wear when compared to linear regression model for all test conditions.

The global optimal solution of selected tool geometry parameters is obtained using particle swarm optimization technique and simulated annealing algorithm for the minimization of flank wear. It is found from the experimental analysis that the percentage improvement in the reduction of flank wear using PSO and SAA are 12.14% and 16.14% respectively.

The results of the non traditional optimization techniques show that simulated annealing algorithm using non-linear regression model gives a comparatively better combination of cutting tool geometry parameters to obtain minimum flank wear when compared with the results of particle swarm optimization technique followed by Taguchi's DoE.

References

1 Thiele J D, Melkote S N, Peascoe R & Watkins T R, *Trans ASME*, 122 (2000) 642-649.
2 Hughes J I, Sharman A R & Ridgwayk C, *Proc Inst Mech Eng Part B: J Eng Manuf*, 220(2) (2006) 93-107.
3 Nalbant M, Altin A & Gokkaya H, *Mater Des*, 28 (4) (2007) 1334-1338.
4 Zhou Li, *Machining Chip-Breaking Prediction with Grooved Inserts in Steel Turning*, Ph. D. Thesis, (2001) 4-6.
5 Al-Zkeri I, Rech J, Altan T, Hamdi H & Valiorgue F, *Int Mach Sci Technol*, 13 (1) (2009) 36-51.
6 Baldoukas A K, Soukatzidis F A, Demosthenous G A & Lontos, A E, *Experimental investigation of the effect of cutting depth, tool rake angle and workpiece material type on the main cutting force during a turning process*, 3rd Int Conf Manufacturing Engineering (ICMEN), Chalkidiki, Greece, Oct 2008, 47-55.
7 Neseli Suleyman, Yaldiz Suleyman & Turkes Erol, *Measurement*, 44(3) (2011) 580-587.
8 Singh Dilbag & Venkateswara Rao P, *Int J Mater Manuf Process*, 22(1) (2007) 15-21.
9 Choudhary Atul & Chauhan Sant Ram, *Int J Mach Mach Mater*, 13(1) (2013) 17-33.
10 Leonardo R Silva & Paulo Davim J, *J Compos Mater*, 43(23) (2009) 2793-2803.
11 Bhattacharyya S K, Jawaid A, Lewis M H & Wallbank J, *Int J Mater Sci Technol*, 10(1) (1983) 482-489.
12 Barry J & Byrne G, *Wear*, 247(2) (2001) 139-151.
13 Kharis Samir K & Lin Y J, *Wear*, 262(1-2) (2007) 64-69.
14 Roland Meyer, Jens Kohler & Berend Denkena, *Int J Adv Manuf Technol*, 58 (2012) 933-940.
15 Singh Virender & Khan Tasmeem Ahmad, *Int J Sci Eng Technol*, 2(7) (2013) 626-630.
16 Farhad Kolahan, Mohsen Manoochehri & Abbas Hosseini, *World Acad Sci, Eng Technol*, 50 (2011) 704-707.
17 Kadirgama K, Abou-El-Hossein K A, Noor M M, Sharma K V & Mohammad B, *Wear*, 270 (2011) 258-268.

18 Yang S H & Natarajan U, *Int J Adv Manuf Tech*nol, 49 (2010) 773-784.
19 Bharathi Raja S & Baskar N, *Int J Adv Manuf Technol*, 54 (2011) 445-463.
20 Vijayakumar K, Prabhaharan P, Asokan R & Saravanan M, *Int J Machine Tools Manuf*, 43 (2003) 1633-1639.
21 Milfelner M, Zuperl U & Cus F, *Int J Simul Model*, 3(2004) 121-131.
22 Ramon Quiza Sardinas, Marcelino Rivas Santana & Eleno Alfonso Brindis, *Eng Appl Artific Intell*, 19 (2006) 127-133.
23 Asokan P, Baskar N, Babu K, Prabhaharan G & Saravanan R, *ASME J Manuf Sci Eng*, 127 (2005) 885-892.
24 Antonio C A, Conceicao & Davim J Paulo, *Ind Lub Tribol*, 57(6) (2005) 249-254.
25 Davim J Paulo, Gaitonde V N & Karnik S R, *J Mater Process Technol*, 205(1-3) (2008) 16-23.
26 Nandi Arup Kumar, *Stat Comput Tech Manuf*, (2012) 145-185.
27 Kanthababu M, *Comput Methods Optimiz Manuf Technol*, (2012) 44-66.
28 Gaitonde V N, Karnik S R & Davim J Paulo, *J Mater Eng Performance*, 18(3) (2009) 231-236.
29 Campos P H S, Ferreira J R, de Paiva A P, Balestrassi P P & Davim J P, *Rev Adv Mater Sci*, 34 (2013) 141-147.
30 Ilhan Asilturk & Harun Akkus, *Measurement*, 44 (2011) 1697-1704.
31 Kingston Barnabas J & Tamizharasan T, *J Inst Eng (India) Ser C*, 93(2) (2012) 133-139.
32 Harry Frank & Steven C Althoen, *Statistics Concepts and applications,* (Cambridge Low Price Edition), 1995, 730-743.
33 Tamizharasan T, Kingston Barnabas J & Pakkirisamy V, *J Eng Manuf*, 93(2) (2012) 133-139.
34 Gaitonde V N, Karnik S R & Davim J Paulo, *Comput Methods Optimiz Manuf Technol*, (2012) 144-161.